Energy Levels in Cl^{34} from the $S^{33}(He^3, d)Cl^{34}$ Reaction: A Study of the $(d_{3/2})^2$ and the $d_{3/2}f_{7/2}$ Interactions*

J. R. Erskine
Argonne National Laboratory, Argonne, Illinois 60439

and

D. J. Crozier and J. P. Schiffer
Argonne National Laboratory, Argonne, Illinois 60439 and University of Chicago, Chicago, Illinois 60637

and

W. P. Alford
University of Rochester, Rochester, New York 14627

(Received 7 December 1970)

The energy levels of Cl^{34} have been studied with the $S^{33}(He^3, d)Cl^{34}$ reaction induced by the 14-MeV He^3 beam of the Argonne tandem Van de Graaff accelerator. An Enge split-pole magnetic spectrograph was used to record the deuteron spectra at scattering angles of 10–65° in 5° steps. An over-all energy resolution width of 17 keV was achieved. 26 levels up to an excitation energy of 4.6 MeV were observed and their spectroscopic factors were extracted. The results, when combined with previously known spin information, enable us to locate the major components of $(d_{3/2})^2$ and $d_{3/2}f_{7/2}$ configurations. The two-body matrix elements obtained here are compared with other two-body data in nearby nuclei and with calculated matrix elements.

I. INTRODUCTION

The nucleus Cl^{34} can be described as a proton and a neutron coupled to the core of S^{32}. Its spectrum should be comparatively simple and easy to interpret; it certainly merits careful experimental study.

Cl^{34} is not an easy nucleus to study experimentally, and only recently have the spins and parities of more than just a few states been measured. Investigations of the $S^{33}(p, \gamma)Cl^{34}$ reaction[1,2] made considerable headway in identifying the spins and parities of states in Cl^{34}. Additional information on spins and configurations in Cl^{34} has been gained in several very recent studies with the $(He^3, p\gamma)$,[3] $(\alpha, n\gamma)$,[4] (d, α),[5] and (p, d)[6] reactions.

The properties of the (He^3, d) reaction in this region of nuclei have been well studied. In particular, a study[7] of the reaction $S^{32}(He^3, d)Cl^{33}$ showed that the $\frac{3}{2}^+$ ground state and a $\frac{7}{2}^-$ excited state in Cl^{33} were good single-particle states; other levels were much weaker.

In the present $S^{33}(He^3, d)Cl^{34}$ experiment, a magnetic spectrograph was used to give good particle identification and energy resolution, and the bombarding energy was close to that used in the previous study on the $S^{32}(He^3, d)Cl^{33}$ reaction. The only major problem was in the acquisition of a suitable S^{33} target.

II. EXPERIMENTAL PROCEDURE

An Enge split-pole magnetic spectrograph[8] was used in conjunction with the beam from the Argonne FN tandem Van de Graaff accelerator. Nuclear track emulsions, covered with enough cellulose triacetate foil to stop all α particles, were used in the focal plane of the spectrograph. The emulsion was scanned with the Argonne automatic plate scanner.[9]

12 exposures were made at scattering angles from 10 to 65° in 5° steps. The data had an energy resolution width of about 17 keV. The resulting spectra were fitted with the program AUTOFIT.[10]

Sulfur is not an easy target material to work with. The elemental form of sulfur is difficult to use as a target because the material quickly evaporates when struck by the beam. One needs to bind the sulfur by combining it with some other material which will not interfere with the experiment. We chose cadmium since its atomic number is high enough that the yield of the (He^3, d) reaction would not be significant at the bombarding energy needed to study the $S^{33}(He^3, d)Cl^{34}$ reaction. Furthermore CdS is a fairly stable material. For the present experiment, 10 mg of sulfur enriched to 83% in S^{33} was obtained from the Isotopes Division of Oak Ridge National Laboratory. To make efficient use of this small sample, the CdS targets were prepared by a modification of the method described by Morrison.[7] A tubular tantalum boat was divided into two sections by a pinch. About 0.8 mg of S^{33} was loaded into one section and about 2.5 mg of cadmium metal was loaded into the other. A hole 1 mm in diameter was drilled into the section con-

taining the sulfur. Several targets about 50-$\mu g/cm^2$ thick were prepared as follows. First the sulfur was evaporated onto a carbon backing which had not been removed from a glass slide. Immediately thereafter, and without opening the evaporator to the atmosphere, the cadmium metal was evaporated on top of the sulfur. While still in the vacuum, the glass slide was heated to 400-500°C for 15–20 min to convert the material to CdS. A change in color and texture indicated that the conversion was complete. The CdS layer was nonuniform; the resolution width in the (He^3, d) data was much larger than would be expected with a uniform layer of CdS 50-$\mu g/cm^2$ thick.

A solid-state detector was used to monitor the target during each of the exposures, with a single-channel analyzer set to count the He^3 particles elastically scattered from the cadmium in the target. Several targets were tested with the spectrograph by recording deuterons elastically scattered from the sulfur and the cadmium. These tests established that the ratio of sulfur to cadmium was the same for all targets tested. Consequently we assumed that the target was indeed CdS and thus that the number of sulfur atoms on the target was exactly equal to the number of cadmium atoms.

Absolute differential cross sections were measured through the use of the He^3 particles elastically scattered from the cadmium in the target and recorded by the monitor counter. On the basis of optical-model calculations with several sets of potential parameters, the elastic scattering cross section was assumed to be 0.83 ± 0.08 times Coulomb scattering. The best positions of the observed peaks along the focal plane were determined by the program AUTOFIT. Since the ground-state transitions were weak in most of the spectra the excitation energies at each angle were computed with reference to the 147-keV state. The energy of this state was determined by Graber and Harris[2] as 146.8 ± 1.0 keV. The energies of the next two states were determined with considerably better accuracy as 461.5 ± 0.3 and 664.6 ± 0.3 keV. The averaged excitation energies were therefore adjusted to best fit those values. The spectrograph had previously been calibrated with α particles from Po^{210} with an assumed energy of 5304.5 keV.

III. EXPERIMENTAL RESULTS

The spectrum of deuterons recorded at 20° is shown in Fig. 1. A few contaminant groups from

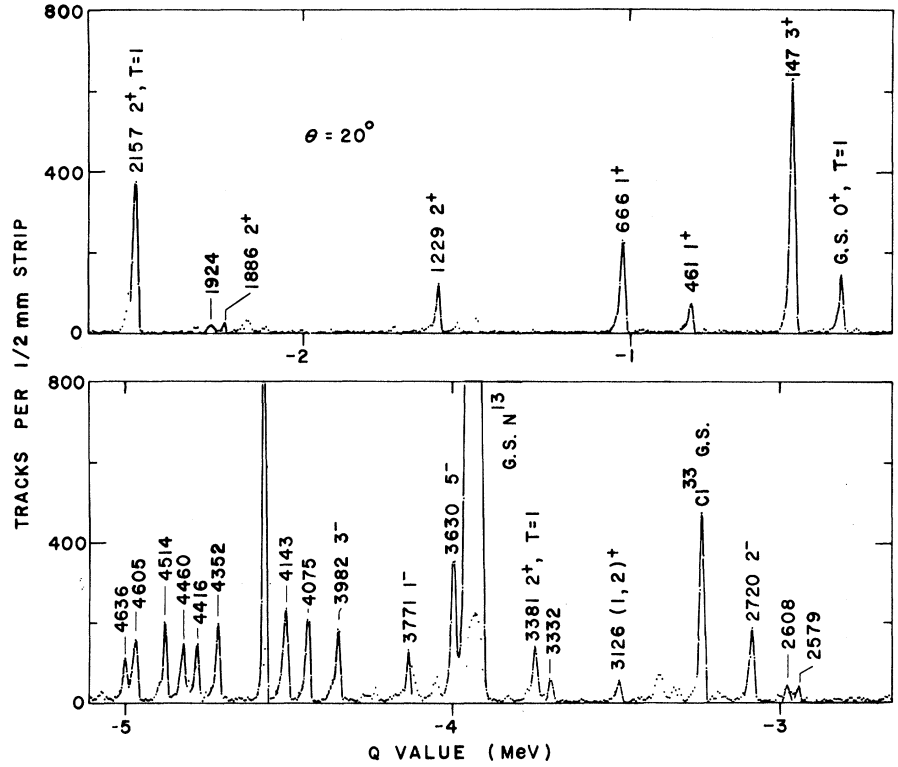

FIG. 1. Spectrum for the split-pole spectrograph. The peaks with lines drawn through them have been identified as indicated by the labels. The spins are those of the present work, from Table II. The weak peaks with no lines through them do not correspond to states in Cl^{34}. The unlabeled peak at about 4.2 MeV is from the $C^{12}(He^3,p)N^{14}$ reaction.

the carbon and oxygen in the target can be seen in the spectrum. The Cl^{33} ground-state group is also present due to the 16% abundance of S^{32} in the target material. In Figs. 2–6 are collected the angular distributions measured in the present study. As can be seen, it is not difficult to distinguish between the different possibilities when the transition is not of mixed l. The agreement between the measured and calculated angular distributions is quite good for the $l=1$ and $l=3$ cases. For $l=0$ and $l=2$ the positions of the maxima are in excellent agreement but the measured minima, as is usual, are not as deep as the distorted-wave (DW) calculation predicts. Table I lists the optical-model parameters used in the DW calculations, which were done with program JULIE.[11]

The excitation energies derived from our (He^3, d) data are presented in Table II. The errors listed are rms averages of the sets of energies given by the spectrum-fitting program. A slightly different set of excitation energies are given in Table III and throughout the rest of this paper. These are the adopted best energies in our opinion, based on our (He^3, d) results together with other measurements.[1–6] Spectroscopic factors for the levels in Cl^{34} measured in this study are presented in Table III. The last column in the table shows our assignment of spins and parities for the levels. Some of these spins have been taken from work cited above. Where necessary for spin assignments, the γ-decay properties are also included. An energy-level diagram of Cl^{34} is given in Fig. 7.

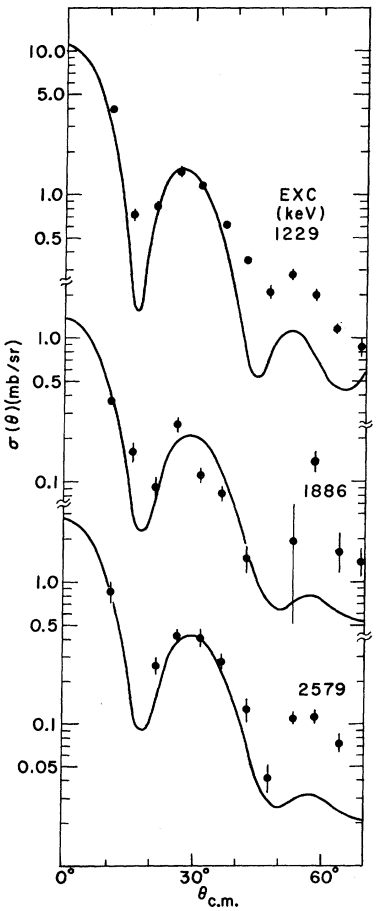

FIG. 2. Angular distributions identified as $l=0$. The lines are DWBA calculations.

TABLE I. Optical-model parameters (from Ref. 7) used in the DWBA calculations.

Incident particle	V (MeV)	W[a] (MeV)	R_0 (F)	a (F)	R_0' (F)	a′ (F)	R_c (F)
He^3	173	18.6	1.07	0.795	1.657	0.762	1.40
d	179.7	26.3	0.656	1.086	1.488	0.535	1.30

[a] Volume absorption was used in the He^3 potential, surface absorption in the deuteron potential.

IV. SPIN ASSIGNMENTS

First of all we examine the spectroscopic information that can be deduced from the (He^3, d) experiment. Values of $G \equiv [(2J_f+1)/(2J_i+1)]\,C^2S$, where $C^2=\frac{1}{2}$ is the isospin coefficient, J_f and J_i are the final and initial spins, respectively, and S is the spectroscopic factor, were extracted from the data by our distorted-wave Born-approximation analysis and are listed in Table III. One simple test we can immediately apply is to sum the values of G for each l value and compare the summed values with the results Morrison[7] obtained in his $S^{32}(He^3, d)Cl^{33}$ experiment. This is done in Table IV. If the coupling of the single-proton states as seen in Cl^{33} to the $\frac{3}{2}^+$ ground state of S^{33} is indeed simple, and if the resultant splitting is within the range of excitation of the present experiment, further analysis is meaningful. Figure 8 is an energy-level diagram for Cl^{33}. In Cl^{34} both $T=0$ and $T=1$ states can be

TABLE II. Excitation energies in keV based on the (He^3, d) data.

145.5	3544.9 ± 2.5
461.0 ± 1.2	3631.4 ± 2.5
665.1 ± 1.4	3773.0 ± 2.4
1229.4 ± 1.6	3983.4 ± 2.5
1885.1 ± 2.9	4076.1 ± 3.2
1923.3 ± 1.7	4145.8 ± 2.7
2157.5 ± 1.5	4353.0 ± 3.0
2579.1 ± 1.6	4418.1 ± 2.8
2608.5 ± 1.3	4460.9 ± 3.4
2720.7 ± 2.5	4516.3 ± 2.2
3128.0 ± 2.2	4607.9 ± 2.1
3333.0 ± 2.4	4638.7 ± 2.1
3382.7 ± 2.0	

populated in the He^3, d reaction. For $l=2$ transitions it is clear that most of the $T=0$ and 1 strengths are observed. For $l=0$, 1, and 3 transitions, the summed strengths are close to those expected for the $T=0$ states alone. With the isospin splitting about 2.5 MeV, this seems to be reasonable.

Having established that the sums are indeed comparable, we can examine the spectroscopic factors in more detail. The absolute values of G are, of course, somewhat uncertain and depend on details of the DW analysis. We choose to renormalize the spectroscopic factors in such a way that their sums are equal to the sum-rule limit, which is nearly equivalent to renormalizing it to the $S^{32}(He^3, d)Cl^{33}$ cross sections. In other words, we wish to study the coupling of the $d_{3/2}$ neutron in S^{33} to the various single-particle states in Cl^{33}. To the extent that these states are not single-particle states, we are studying the coupling of the more complex configurations which are the best candidates for single-particle states, and arguments on whether these are the "true" single-particle states in some idealized shell-model representation are largely irrelevant to our analysis. The renormalized G' values are listed in Table V. The total strength for each final spin within each multiplet must then be in proportion to $(2J_f+1)$. The expected strengths are listed in Table VI.

We consider first the $l=2$ transitions. The values of J^π, T are known to be 0^+, 1 for the ground state and 3^+, 0 for the 147-keV first excited state. They approximately exhaust the sum rule for these transitions. The known 1^+ states at 461 and 666 keV have nearly the full 1^+ strength given in Table VI. The 2157- and 3381-keV states were both assigned as 2^+, $T=1$ analogs of states in S^{34}. Their summed strength comes to about 90% of the expected 2^+ strength. Of the remaining states that show weak $l=2$ transitions, we can put no restrictions on the 1924-keV state; the 2608-keV state is observed to have a 40% decay branch to the 3^+ state and hence is not 0^+ but could be 1^+, 2^+, or 3^+; the 3126-keV state was observed to decay entirely to the 0^+ ground state, so it should be 1^+ or 2^+; and no restriction can be put on the 3332-keV state. It

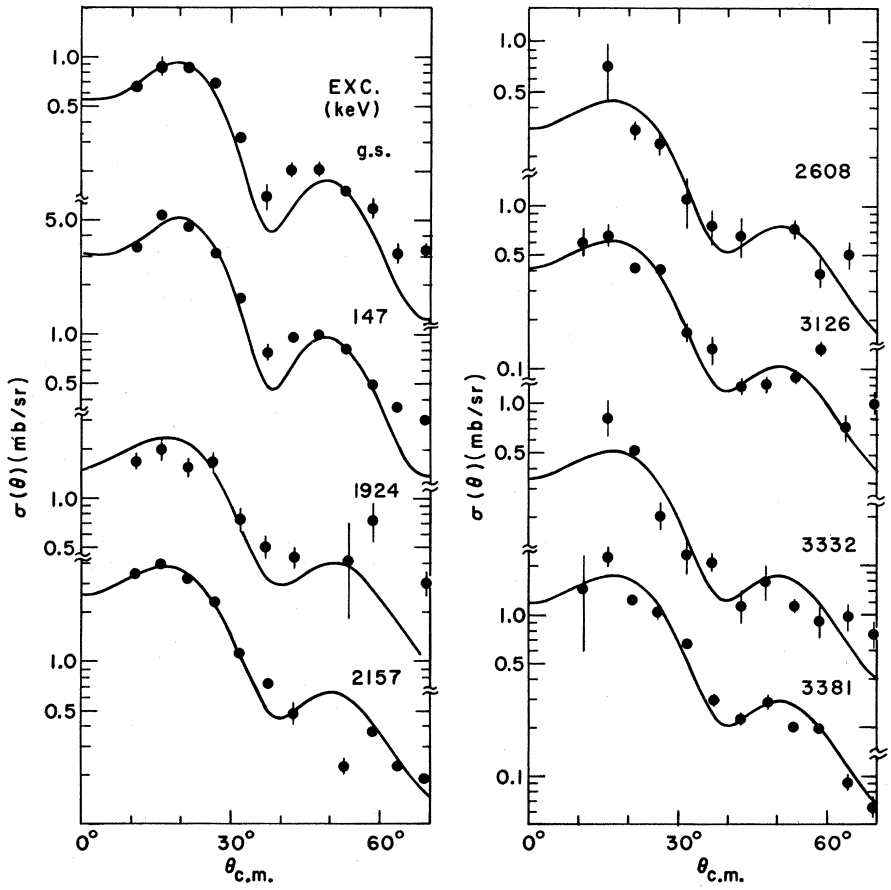

FIG. 3. Angular distributions identified as $l=2$ transitions. The lines are DWBA calculations.

should be remarked that since none of these states appear to have analogs in S^{34}, they are presumably $T=0$ and thus are more likely to admix with the $T=0(d_{3/2})^2$ states which are, of course, 1^+ and 3^+. Isospin-violating matrix elements are generally no greater than 100 keV; thus admixtures for 2^+ states are possible, but for 0^+ states they are very unlikely. We indicate this in Table III by omitting the possibility of $J^\pi=0^+$ and writing the J values for $T=0$ configurations first. The summed strengths for $l=2$ transitions are displayed graphically in Fig. 9.

For the states to which $l=0$ transitions are seen, we have already mentioned the two 1^+ states that show mixed $l=2$ and $l=0$ transitions. Since the 1229-keV state was previously assigned as $J=2$, and the $l=0$ angular distribution establishes the parity as even, it follows that $J^\pi=2^+$. The 1886-keV state has previously been assigned 2^+; and the 2579-keV state, previously assigned $J=1$, is now shown to be $J^\pi=1^+$.

For the $l=3$ transitions, we observe first of all

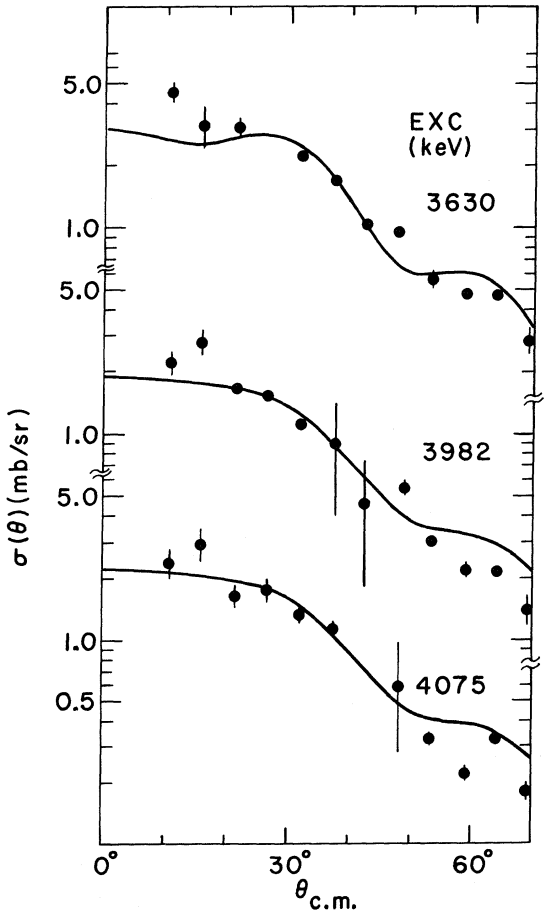

FIG. 4. Angular distributions identified as $l=3$ transitions. The lines are DWBA calculations.

in Table III that the sum of spectroscopic strengths is 3.54 as compared to the expected 3.60 from $S^{32}(He^3, d)Cl^{33}$. Thus it seems unlikely that we would have missed an appreciable fraction of the $T=0$ $l=3$ transition strength. The 2720-keV state has been previously assigned $J=2$. We can say that it is $J^\pi=2^-$ and that it exhausts the sum-rule limit. The 3630-keV state is too strong to be anything but the $J^\pi=5^-$ state. The 3982- and 4075-keV states are about equal in strength and about right for $J^\pi=3^-$ and 4^-. The former decays to the 2^+ and 3^+ states and therefore is most likely the 3^- member, so the 4075-keV state is left as 4^-. The 4143-keV state appears to be reached by a mixed $l=1$ and $l=3$ transition. This restricts the spin to 2^- or 3^-. The $l=3$ strength of this state favors a 3^- assignment. The γ decay of Ref. 1 appears to be entirely to the ground state which is rather strange. Perhaps, since this was a NaI experiment, the possibility of decay to the 147-keV 3^+ state should not have been ruled out. The strengths for $l=3$ transitions are plotted in Fig. 10.

For the $l=1$ states the strength is fragmented, so it is not possible to assign any spins. The 3544-keV state is observed to decay entirely to the 3^+ state and hence is likely to be 2^- or 3^-. The 3771-keV state decaying to the 0^+ ground state must be 1^-. The 4352-, 4416-, and 4460-keV states are all too strong to be 0^-, but otherwise no restrictions can be put on their spins. The γ decay from the 4514- and 4605-keV states to the 3^+ states restricts them to 2^- or 3^-. Finally, we assign 0^- to the 4636-keV state. We feel reasonably confident in this assignment since: (a) The summed $l=1$ strength is close to the expected value and (b) the 0^- state is rather unique and it is difficult to make up additional 0^- states in this energy vicinity into which the strength could be fragmented. Thus, since the 4636-keV state is the only $l=1$ state with a weak enough spectroscopic strength to be 0^- it has a reasonably high probability of being correctly assigned.

V. TWO-BODY MATRIX ELEMENTS

Since we identify the major components of the $(d_{3/2})^2$ and $d_{3/2}f_{7/2}$ spectra, it is of interest to obtain the matrix elements of this interaction from our data. When the strength to a state of given J is fragmented, the matrix elements can be obtained by computing the centroid of all these states in a multiplet and estimating the uncertainties caused by the weak unassigned states of each l. To quote the matrix elements of the residual interaction, we must measure them with respect to the energy at which a two-body multiplet would occur if there were no residual interaction. For the $(d_{3/2})^2$ multi-

plet we obtain this from the binding energies of the $\frac{3^+}{2}$ ground states in S^{33} and Cl^{33} by writing

$$E_R = M(S^{32}) + M(p) + M(n) + Q[S^{32}(p,\gamma_0)Cl^{33}] + Q[S^{32}(n,\gamma_0)S^{33}] - (MCl^{34})$$
$$= 2.867\ \text{MeV excitation in } Cl^{34}.$$

For the $(d_{3/2}f_{7/2})$ multiplet, the excitation energy is

$$E_R = M(S^{32}) + M(p) + M(n) + \tfrac{1}{2}[Q(S^{32}(p,\gamma_0)Cl^{33}] + Q[S^{32}(n,\gamma_0)S^{33}] + Q[S^{32}(p,\gamma_f)] + Q[S^{32}(n,\gamma_f)] - M(Cl^{34}) = 5.681\ \text{MeV},$$

where $Q(p,\gamma_f)$ refers to the Q value for the capture reaction leading to the $\frac{7}{2}^-$ state in mass 33, and $M(\ )$ is the mass in MeV of the indicated entity.

The matrix elements for $(d_{3/2})^2$ may be compared with the data[12] on K^{38}. This is done in Fig. 11. A comparison with other $(d_{3/2})^2$ matrix elements in the literature is made in Table VII. The hole-hole interaction in K^{38} should be identical to the particle-particle interaction in Cl^{34}, other things being equal. The uncertainty in K^{38} arises from the fact that in the $K^{39}(d,t)K^{38}$ reaction one cannot distinguish between $l=2$ pickup of $d_{3/2}$ and $d_{5/2}$ neutrons; so admixtures in these states cannot be ruled out. This difficulty does not enter into our Cl^{34} experiment.

Considerable data exist on the $d_{3/2}f_{7/2}$ interaction. Pandya[13] and Goldstein and Talmi[14] showed 15 years ago that the low-lying spectra of Cl^{38} and K^{40} were related by a simple Racah transformation which one would expect to hold in the simplest jj-coupling shell model. This is called the Pandya transformation and may be written[15] as

$$E_J^{p-h(p-p)}(n-p) = -\sum_{J'} W(j_1 j_2 j_2 j_1; JJ') E_{J'}^{p-p(p-h)}(n-p). \quad (1)$$

Here p – h (p – p) is used to indicate particle-hole (or particle-particle) matrix elements, and $(n-p)$ refers to the neutron-proton, mixed isospin case. The E_J represent the energy matrix elements. Figures 12(a) and 12(b) are diagrammatic representations of Cl^{38} and K^{40}; the Cl^{38} spectrum is the

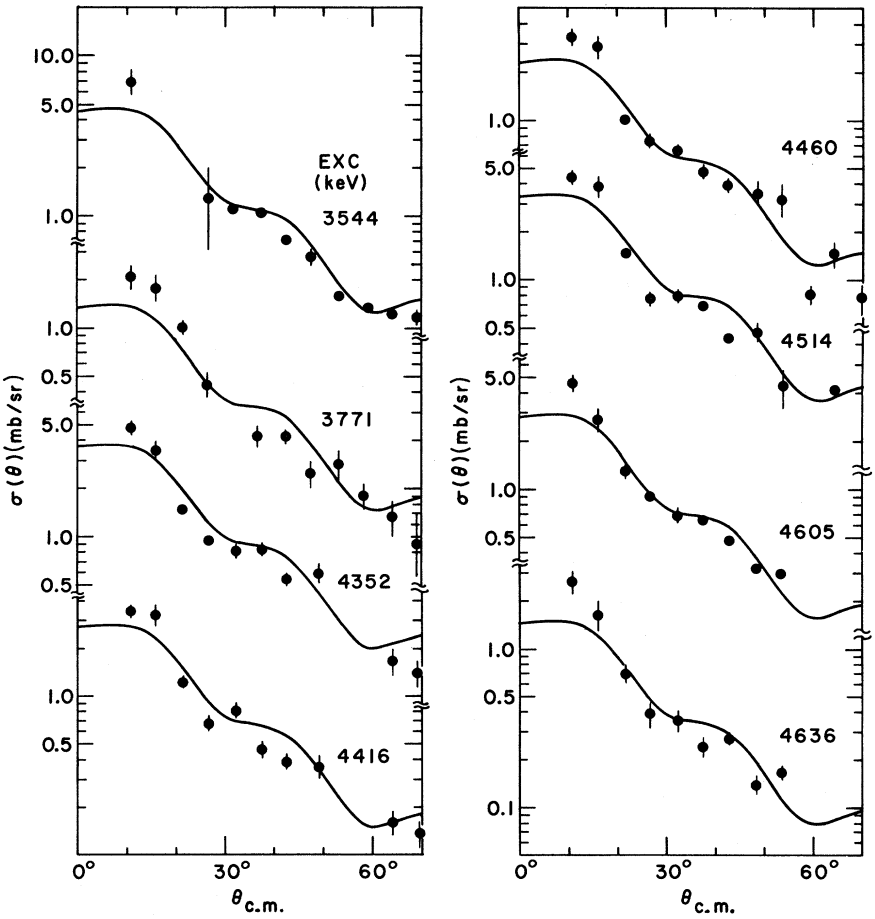

FIG. 5. Angular distributions identified as $l=1$ transitions. The lines are DWBA calculations.

TABLE III. Summary of spectroscopic strengths and spin assignments.

Excitation energy (keV)	$G=[(2J_f+1)/2J_i+1)]\,C^2S$ $l=0$	$l=1$	$l=2$	$l=3$	Spin and parity assignments from other work	γ-decay branching [a]	Present spin and parity assignments
0			0.25		0^+		0^+
147			1.42		3^+		3^+
461	0.04		0.08		1^+ [b,c]		1^+
666	0.07		0.50		1^+ [c–f]		1^+
1229	0.12				2 [b]		2^+
1886	0.02				2^+ [b]		2^+
1924			0.04				$(1, 3, 2)^+$
2157			0.66		2^+ [b,f]		2^+
2579	0.03				1 [d,c]		1^+
2608			0.08			To 1^+, 2^+, (3^+) [c,g]	$(1, 3, 2)^+$
2720		0.04		0.39	2 [d]		2^-
3126			0.11		1^+ [c]	All to 0^+ [g,h]	$(1, 2)^+$
3332			0.09				$(1, 3, 2)^+$
3381			0.31		2^+ [c,f]		2^+
3544		0.18				All to 3^+ [e,h]	2^-, 3^-
3630				1.10			5^-
3771		0.05				All to 0^+ [h]	1^-
3982				0.44		To 3^+ & 2^+ [e]	3^-
4075				0.52			4^-
4143 [i]		0.08		0.24		All to 0^+ [h]	$3^-(2^-)$
4352		0.14					$(1-3)^-$
4416		0.11					$(1-3)^-$
4460		0.09					$(1-3)^-$
4514		0.13				All to 3^+ [h]	$(2-3)^-$
4605		0.11				All to 3^+ [h]	$(2-3)^-$
4636		0.06					0^-, $(1, 2, 3)^-$

[a] Listed only for levels for which no spin assignments were available from γ-ray work; only the data relevant to spin assignments are given. In case of conflicting data, only the results which seemed the most reliable are listed.

[b] Brandolini *et al.*, Ref. 3.

[c] DeLuca, Lawson, and Chagnon, Ref. 3.

[d] Sykes, Ref. 3.

[e] Graber and Harris, Ref. 2.

[f] Brunnader, Hardy, and Cherny, Ref. 5.

[g] Horoshko and Shapiro, Ref. 5.

[h] Glaudemans, Eriksson, and Werkhoven, Ref. 1.

[i] *Note added in proof:* The 4119-keV (2^+) state in S^{34} has been seen in preliminary results from a $S^{33}(d,p)S^{34}$ experiment with a mixed $l=0$ and $l=2$ angular distribution. This suggests that the 4143-keV state in Cl^{34} is the analog, that the (He^3,d) angular distribution appears to be consistent, and that the spin assignment should be changed to $(2^+, T=1)$.

TABLE IV. Summed strengths.

l	Predicted [a]	Observed
0	$\frac{1}{2}\times 0.58 = 0.29$ [b]	0.28
1	$\frac{1}{2}\times 2.20 = 1.10$ [b,c]	0.99
2	3.60	3.54
3	$\frac{1}{2}\times 5.84 = 2.92$ [b]	2.69

[a] From the results of the $S^{32}(He^3, d)Cl^{33}$ experiment (Ref. 7).

[b] The factor $\frac{1}{2}$ represents the assumption that only $T=0$ states were included in the present work.

[c] A single $l=1$ state (presumably $\frac{3}{2}^-$) was seen in Ref. 7.

TABLE V. Renormalized strengths G'.

$l=1$ E_x (keV)	G' [a]	$l=2$ E_x (keV)	G' [b]	$l=3$ E_x (keV)	G' [a]
2720	0.08	0	0.28	2720	0.57
3544	0.37	147	1.60	3630	1.64
3771	0.10	462	0.09	3982	0.65
4143	0.16	665	0.57	4075	0.78
4352	0.28	1924	0.05	4143	0.36
4416	0.22	2158	0.75		
4460	0.18	2608	0.09		
4514	0.27	3126	0.12		
4605	0.22	3332	0.10		
4636	0.12	3381	0.35		
$\sum G$	2.00		4.00		4.00

[a] Renormalized to the total expected strength for $T=0$.

[b] Renormalized to the total expected strength.

TABLE VI. Expected summed strengths.

$l=1$		$l=2$		$l=3$	
J, T	$\sum G$	J, T	$\sum G$	J, T	$\sum G$
0, 0	0.125	0, 1	0.25	2, 0	0.625
1, 0	0.375	1, 0	0.75	3, 0	0.875
2, 0	0.625	2, 1	1.25	4, 0	1.125
3, 0	0.875	3, 0	1.75	5, 0	1.375
Total	2.0		4.0		4.0

TABLE VII. $(d_{3/2})^2$ matrix elements (MeV).

J, T	0, 1	1, 0	2, 1	3, 0
Present work [a]	−2.87	−2.23	−0.32	−2.72
Glaudemans [b]	−2.27	−0.92	+0.16	−2.64
Erné [c]	−1.71	−2.11	+0.26	−2.51

[a] Uncertainties less than ±0.1 MeV.

[b] See Ref. 23.

[c] See Ref. 17.

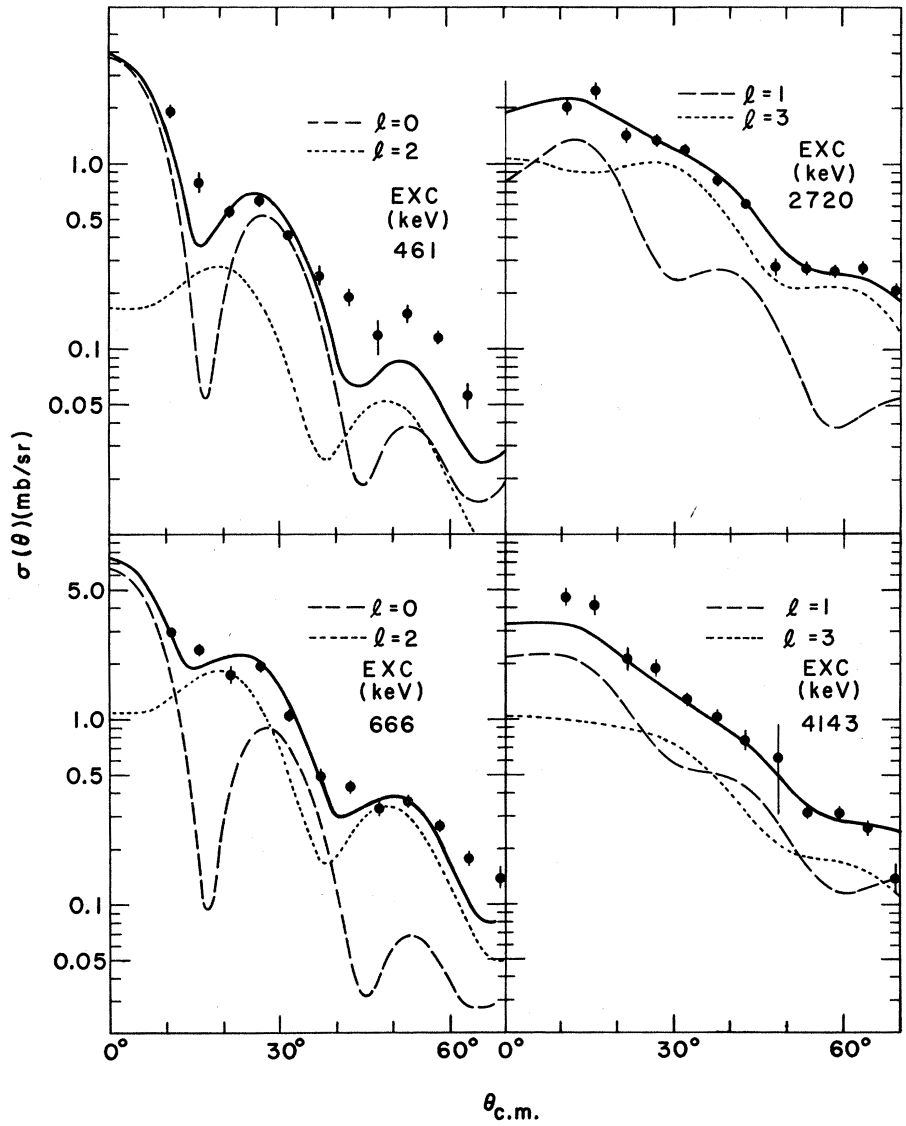

FIG. 6. Angular distributions which were identified as transitions with mixed l values. The dashed lines represent the components with different angular-momentum transfer. The solid lines are the sum of the dashed curves.

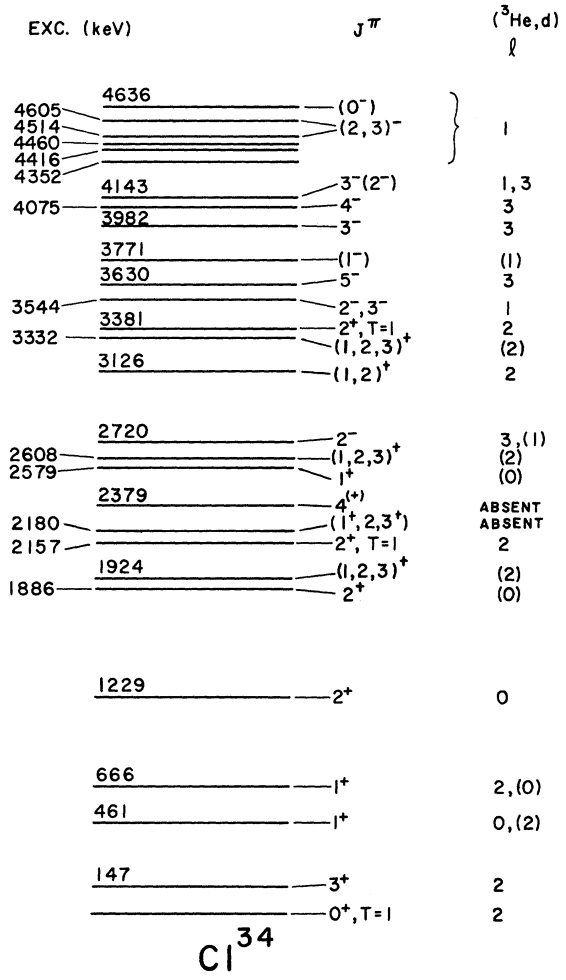

FIG. 7. Energy-level diagram of Cl^{34}.

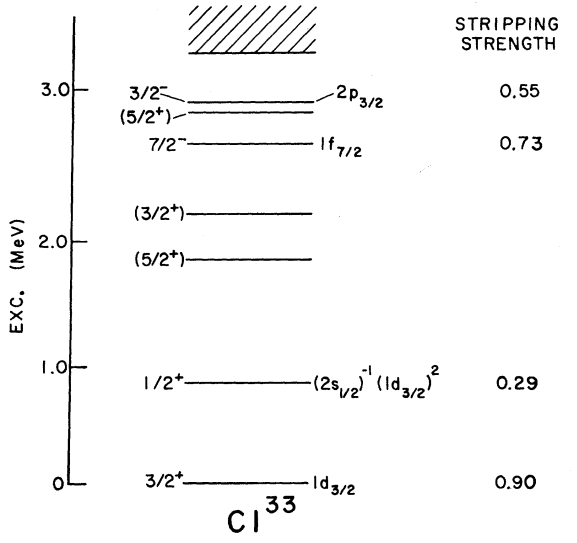

FIG. 8. Energy levels in Cl^{33} from Ref. 7.

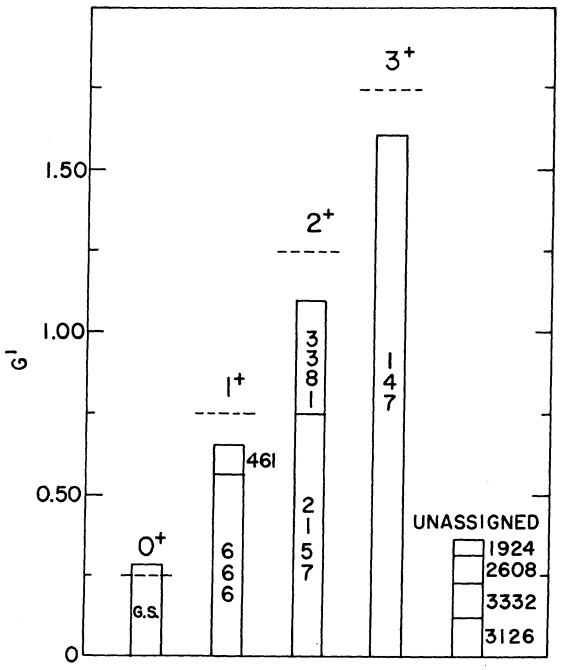

FIG. 9. The spectroscopic strengths G' for $l=2$ transitions. The values expected for various J values are indicated by horizontal dashed lines.

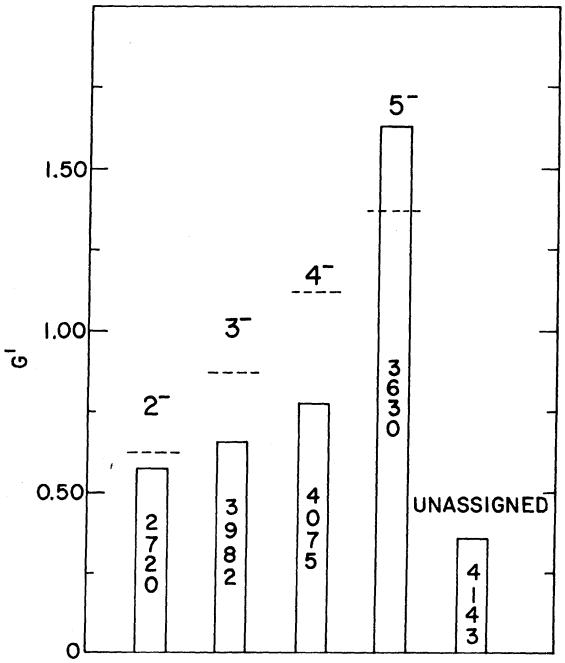

FIG. 10. The spectroscopic strengths G' for $l=3$ transitions. The values expected for various J values are indicated by horizontal dashed lines.

TABLE VIII. $d_{3/2}f_{7/2}$ matrix elements (MeV).

	$T=0$ matrix elements				$T=1$ matrix elements			
	$J=2$	3	4	5	$J=2$	3	4	5
Cl^{34} and Cl^{38}	−2.98	−1.71	−1.61	−2.06	−0.41	−0.16	+0.84	+0.08
Ca^{40} (Ref. 16)	−4.14	−1.92	−2.03	−2.35	+0.91	+0.21	+1.45	+0.52
Moinester and Alford (Ref. 19)	−4.23	−1.89	−2.26	−2.11	+0.64	−0.25	+1.35	−0.08
Erné (Ref. 17)	−3.65	−1.85	−1.77	−2.90	+0.38	−0.08	+0.92	+0.43
Dieperink and Brussaard (Ref. 18)	−4.01	−2.01	−1.87	−2.37	+0.62	−0.07	+0.98	+0.20
Satoris and Zamick (Ref. 20)	−4.75	−1.41	−0.96	−1.73	+0.27	−0.04	+0.81	−0.88
Kuo and Brown (Ref. 21)	−3.11	−1.63	−0.87	−1.29	+0.28	0.07	0.34	−0.59

particle-particle and K^{40} the particle-hole spectrum. Spectra such as these may be referred to as n-p spectra because the orbits are specified for the proton and the neutron. The diagram for Cl^{34} is also shown in Fig. 12(c). From this it is clear that in Cl^{34} there are two possibilities corresponding to two isospin states, while in Cl^{38} and K^{40} the isospin of the two particles is mixed. If we write

$$E_J^{p-h(p-p)}(n-p) = \tfrac{1}{2}[E_{J,T=0}^{p-p\ (p-h)} + E_{J,T=1}^{p-p\ (p-h)}], \quad (2)$$

then the Pandya relation with isospin becomes

$$E_{JT}^{p-p(p-h)} = -\sum_{J',T'}(2J'+1)(2T'+1)W(j_1 j_2 j_2 j_1; JJ') \times W(\tfrac{1}{2}\tfrac{1}{2}\tfrac{1}{2}\tfrac{1}{2}; TT')E_{J'T'}^{p-h(p-p)}. \quad (3)$$

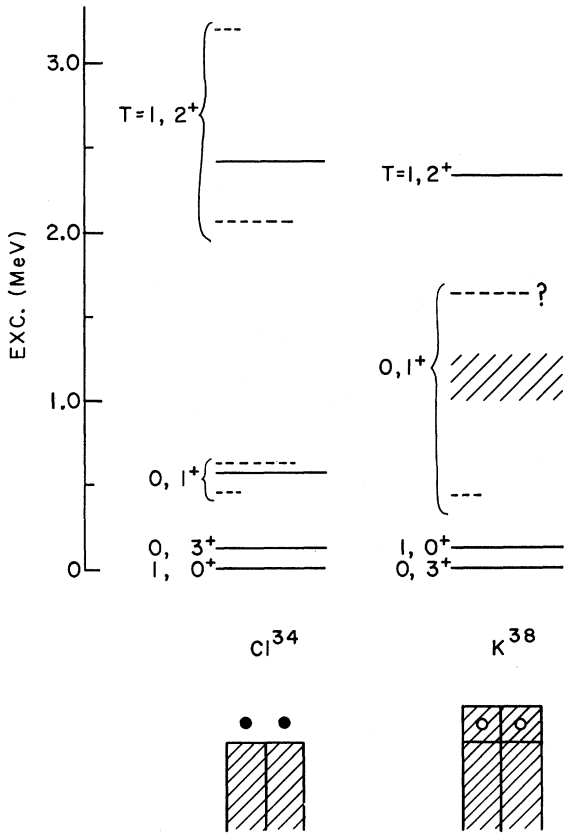

FIG. 11. Comparison of the states identified as belonging to the $(d_{3/2})^2$ states in K^{38} from Ref. 12. A schematic representation of the two nuclei is also shown.

In the present experiment we have determined the matrix elements for $T=0$ in this multiplet and have listed them in Table VIII. We note that the possible confusion in the $J=3$ and 4 assignments introduces an uncertainty of at most 0.1 MeV. Given these $T=0$ matrix elements we can immediately refer to the n-p spectrum of Cl^{38} and can use Eq. (2) to extract the $T=1$ matrix elements as well. These are also given in Table VIII. An alternative source of the complete $d_{3/2}f_{7/2}$ matrix elements is the $d_{3/2}^{-1}f_{7/2}$ spectrum[16] of Ca^{40}. The diagram appropriate to Ca^{40} is also shown in Fig. 12(d). Using Eq. (3), we obtain the matrix elements shown in the second line of Table VIII; the evident discrepancies call for a closer examination.

In the case of the p-h matrix elements for $T=1$, we have an excellent check; they are, in fact, identical to the n-p matrix elements in K^{40}. They represent the isobaric analog of that multiplet, and K^{40} is in turn related to Cl^{38} by the Pandya transformation. As seen from the comparison in Fig. 13 they are very nearly the same; so it seems reasonable to assume that this set of matrix elements is acceptable.

The $T=0$ energies in Ca^{40} can be examined by comparing either the p-p or the p-h matrix elements for $T=0$. As seen in Fig. 14(a), the discrepancy in the p-p states is mostly for $J^\pi = 2^-$. It is difficult to see how the values for Cl^{34} could be grossly in error since this would imply the exis-

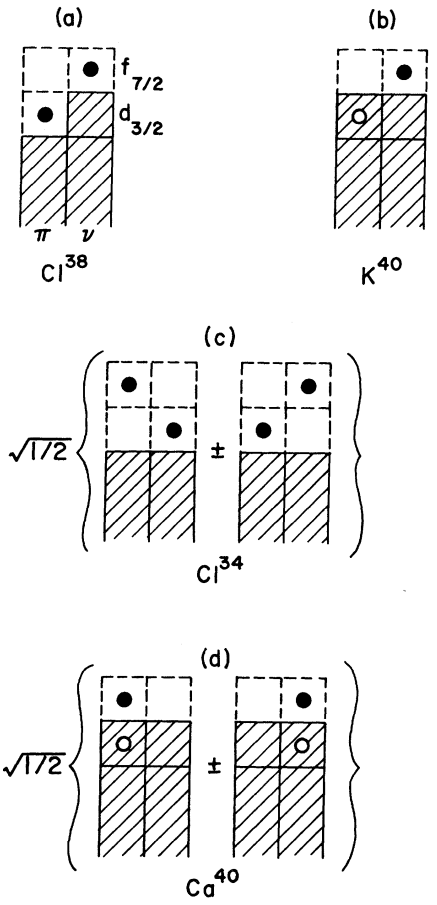

FIG. 12. Schematic representation of different nuclei in which data are available for $d_{3/2}$-$f_{7/2}$ multiplets.

tence of a 2^- state ~1-MeV lower in energy. The alternative comparison [Fig. 14(b)] indicates that the discrepancy may be for the 3^- and 5^- states of Ca^{40}, and this is amenable to a more plausible explanation. In Ca^{40} the lowest 3^- and 5^- states were identified[16] as the members of the multiplet. At the same time these states are known to have strong collective enhancement, with $B(E3)$ and $B(E5)$ to the ground state much larger than single-particle values; it seems reasonable that the collective admixtures would substantially depress these states in energy. We conclude then that the trouble seems to lie in the $T=0$ matrix elements from Ca^{40} and that the matrix elements from Cl^{34}–Cl^{38} are perhaps to be preferred. Our prediction of the $T=1$ $d_{3/2}f_{7/2}$ level scheme in S^{34} or Cl^{34} is given in Table IX.

TABLE IX. Predicted $T=1$ $d_{3/2}f_{7/2}$ excitation energies in S^{34} or Cl^{34}.

J^π	2^-	3^-	4^-	5^-
E_x (MeV)	5.28	5.53	6.53	5.71

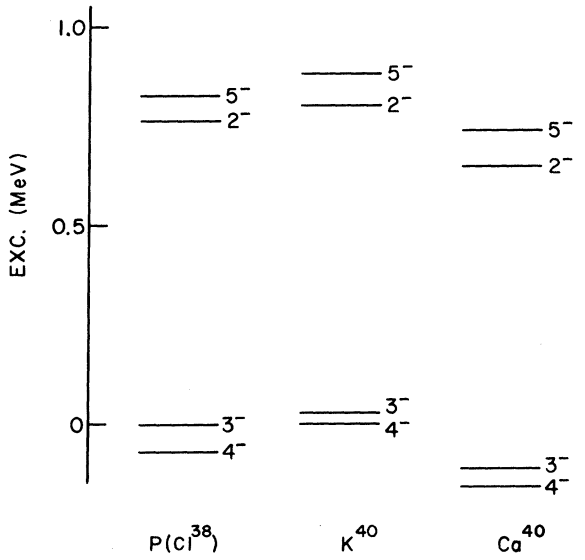

FIG. 13. Comparison of the n-p $d_{3/2}$-$f_{7/2}$ levels in Cl^{38}, K^{40}, and Ca^{40}. The Cl^{38} spectrum has been transformed by the Pandya transformation.

A number of papers[17–19] have reported extracting the best $d_{3/2}f_{7/2}$ matrix elements from all of the previously available data in this region, and other authors[20,21] have calculated these matrix elements from a "realistic" force. These results are compared with the present Cl^{34}-Cl^{38} values in Table VIII. It is clear that it would be of great interest to obtain the $T=1$ matrix elements in mass 34 directly. However, collective admixtures in the 3^- and 5^- states may cause difficulties similar to the ones just mentioned in the case of Ca^{40}.

The multipole matrix elements for a two-body interaction have been defined.[15] An interesting difference has been observed in the quadrupole coefficients extracted from data where the two orbits are identical. For both the $(g_{9/2})^2$ and the $(f_{7/2})^2$ interaction the quadrupole coefficient seemed anomalously large,[22] approximately 50% larger relative to the monopole term than for all other mul-

TABLE X. Multipole matrix elements (MeV).

k	$(d_{3/2})^2$ α_k	α_k [a]	$d_{3/2}f_{7/2}$ γ_{k0} [b]	γ_{k1} [c]	γ_{k1}-γ_{k0} [d]
0	−1.89	−0.93	−2.00	0.14	2.14
1	−0.36	+0.16	0.16	0.15	−0.01
2	−0.97	−0.38	−0.41	−0.37	+0.04
3	−0.21	−0.04	0.14	−0.22	0.36

[a] From Cl^{38}.
[b] From Cl^{34}.
[c] From Cl^{38} combined with Cl^{34}.
[d] This is the same as the coefficient $\alpha_{k\tau}$ for $\tau=1$ defined in Ref. 15.

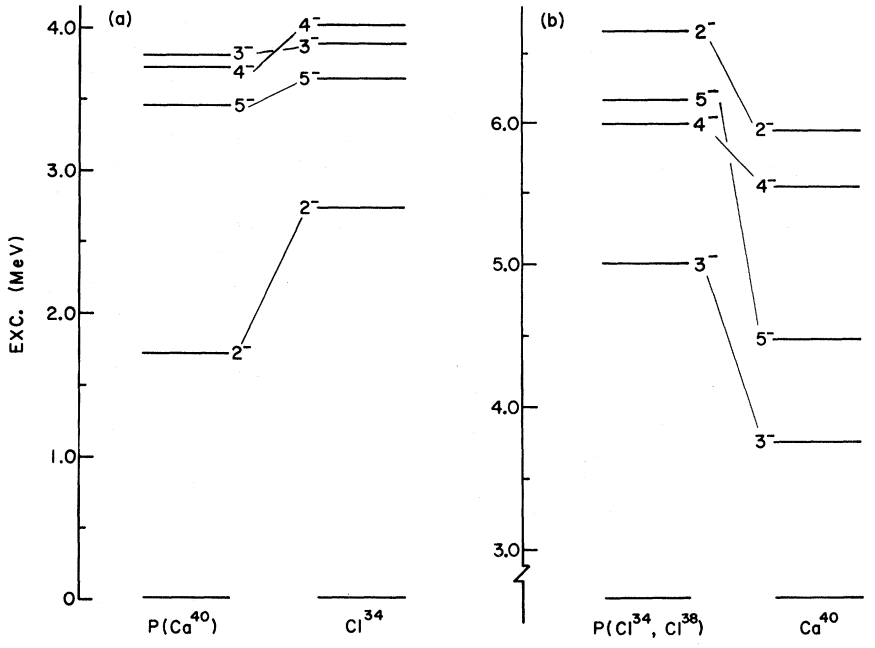

FIG. 14. Comparison between the $d_{3/2}$-$f_{7/2}$ levels of Ca^{40} and Cl^{34}. In the left-hand part of the figure, the Pandya transform of Ca^{40} into $T=0$ energy matrix elements is compared with the Cl^{34} spectrum. The right-hand side shows the $T=0$ particle-hole matrix elements deduced from the combined Cl^{34} and Cl^{38} spectra by the Pandya transformation compared with the $T=0$ Ca^{40} spectra.

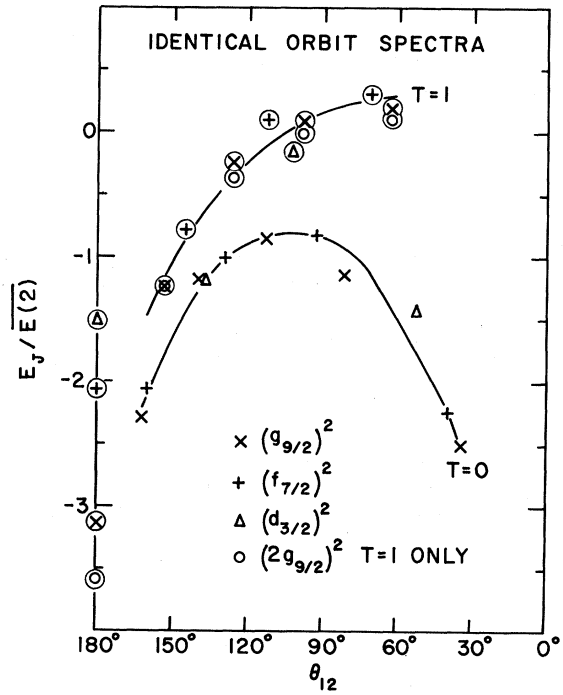

FIG. 15. Comparison of two-body spectra from all known multiplets formed by two particles (holes) in the same orbit. The matrix elements are normalized to the average two-body energy [monopole coefficient or $(2J+1)$ weighted centroid] and θ_{12} is the quantum-mechanical angle between the two orbits. The $T=1$ matrix elements are circled.

tiplets with the orbits nonidentical. The expression for extracting the coefficients of the multipole expansion from a multiplet is given in Ref. 15. The coefficients for the $(d_{3/2})^2$ interaction are shown in Table X. The quadrupole coefficient is 0.51 times the monopole term, whereas it was 0.75 ± 0.05 times the monopole term in the $(f_{7/2})^2$ and the $(g_{9/2})^2$ multiplets. The apparent quadrupole coefficient extracted from a multiplet involving small j values can be substantially lower than the asymptotic value. It was shown in Ref. 15 that for a δ-function interaction the quadrupole coefficient in a $(\frac{3}{2})^2$ spectrum would be some 20% lower than in the limit of large j's. This discrepancy therefore is not serious. To demonstrate this further, we can plot all the identical-orbit spectra as a function of θ_{12}, the angle between the angular momentum vectors $\vec{j}_1$ and $\vec{j}_2$ coupled to a total $\vec{J}$, defined by

$$2[j_1(j_1+1)j_2(j_2+1)]^{1/2}\cos\theta_{12} = J(J+1) - j_1(j_1+1) - j_2(j_2+1).$$

If we divide the matrix elements by the average two-body energy (or monopole coefficients) we see the result in Fig. 15. It is clear that the agreement between the $(d_{3/2})^2$ interaction and the other multiplets with orbits identical is very good, except for the 0^+ states where the matrix elements vary greatly:

For the $d_{3/2}f_{7/2}$ interaction, following the notation of Appendix II of Ref. 15, we can perform a multipole decomposition of the $T=0$ and $T=1$ matrix elements separately. Since this is the first case in which complete data for such nonidentical-orbit multiplets have been obtained, the results are of some interest. The data treated in Ref. 15 were all for mixed-isospin n-p multiplets, and the multipole coefficients indicated remarkably good agreement with a δ-function force. The coefficients for the $d_{3/2}f_{7/2}$ interaction are given in Table X for the mixed-isospin Cl^{38} spectrum, the $T=0$ matrix elements in Cl^{34} obtained in the present experiment, and the $T=1$ matrix elements deduced from combining the Cl^{34} and Cl^{38} information. Following the convention of Ref. 15, we write α_k for the mixed-isospin multipole coefficients and γ_{kT} for the coefficients corresponding to the E_{JT} energy matrix elements. An interesting feature of Table X is that, while the monopole coefficients are quite different, the coefficients for the higher multipoles are remarkably similar. This feature is much more pronounced in the present matrix elements than in any of the earlier ones listed in Table VIII. An equivalent alternative statement is that the relative spacing within the $T=0$ multiplet is similar to that in the $T=1$ multiplet. The interpretation in terms of a two-body interaction would be that the effective interaction appears to be much like a δ-function force which is independent of T, and the isospin-dependent force is of long-range character affecting only the monopole term (centroid) of the multiplets. This long-range effective force cancels in the mixed-isospin n-p spectra so that only the δ-function part is left.

Two shell-model calculations are available for Cl^{34}, one by Glaudemans, Weichers, and Brussaard[23] and the other by Wildenthal.[6] Both calculations agree reasonably well with the observed strong even-parity transitions, except that Glaudemans does not predict two low-lying 1^+ states and he predicts the $l=2$ strength to 1^+ states to be spread to high excitation energies much more than is observed in the data. Wildenthal's unpublished calculation is superior in this regard. No calculations of odd-parity states have been made. The simplicity of the Cl^{34} spectrum implies that the shell-model calculations would be tested mainly in the fitting of small details such as admixtures, since the main features of the spectrum are determined by the two-body matrix elements.

ACKNOWLEDGMENTS

We would like to thank Dr. Dieter Kurath and Dr. R. D. Lawson for very helpful discussions. The assistance of W. Horath in target preparation, of C. Bolduc in the operation of the spectrograph, and of E. Sutter in the operation of the plate scanner is also appreciated.

---

*Work performed under the auspices of the U. S. Atomic Energy Commission.

[1]P. W. M. Glaudemans, L. Eriksson, and J. A. R. Werkhoven, Nucl. Phys. 55, 559 (1964).

[2]H. D. Graber and G. I. Harris, Phys. Rev. 188, 1685 (1969).

[3]D. H. Sykes, Nucl. Phys. A149, 418 (1970); F. Brandolini, I. Filosofo, C. Signorini, and M. Morando, *ibid.* A149, 401 (1970); P. M. DeLuca, J. C. Lawson, and P. R. Chagnon, Bull. Am. Phys. Soc. 15, 566 (1970); and private communication.

[4]F. Brandolini, R. G. R. Engmann, and C. Signorini, Nucl. Phys. A149, 411 (1970).

[5]H. Brunnader, J. C. Hardy, and J. Cerny, Nucl. Phys. A137, 487 (1969); R. N. Horoshko and M. H. Shapiro, Bull. Am. Phys. Soc. 15, 530 (1970); and private communication.

[6]B. H. Wildenthal, G. M. Crawley, and W. McLatchie, Bull. Am. Phys. Soc. 15, 484 (1970); and private communication.

[7]R. A. Morrison, Nucl. Phys. A140, 97 (1970).

[8]J. E. Spencer and H. A. Enge, Nucl. Instr. Methods 49, 181 (1967).

[9]J. R. Erskine and R. H. Vonderohe, Nucl. Instr. Methods 81, 221 (1970).

[10]P. Spink and J. R. Erskine, Argonne National Laboratory Physics Division Informal Report No. PHY-1965B (unpublished); J. R. Comfort, Argonne National Laboratory Physics Division Informal Report, PHY-1970B (unpublished).

[11]R. H. Bassel, R. M. Drisko, and G. R. Satchler, Oak Ridge National Laboratory Report No. ORNL-3240 (unpublished).

[12]H. T. Fortune, N. G. Puttaswamy, and J. L. Yntema, Phys. Rev. 185, 1546 (1969).

[13]S. P. Pandya, Phys. Rev. 103, 956 (1956).

[14]S. Goldstein and I. Talmi, Phys. Rev. 102, 589 (1956).

[15]M. Moinester, J. P. Schiffer, and W. P. Alford, Phys. Rev. 179, 984 (1969).

[16]J. R. Erskine, Phys. Rev. 149, 854 (1966). See also K. K. Seth, J. A. Biggerstaff, P. D. Miller, and G. R. Satchler, *ibid.* 164, 1450 (1967); J. S. Forster, K. Bearpark, J. L. Hutton, and J. F. Sharpey-Schafer, Nucl. Phys. A150, 30 (1970).

[17]F. C. Erné, Nucl. Phys. 84, 91 (1966).

[18]A. E. L. Dieperink and P. J. Brussaard, Nucl. Phys. A106, 177 (1968).

[19]M. A. Moinester and W. P. Alford, Nucl. Phys. A144, 305 (1970).

[20]G. Sartoris and L. Zamick, Phys. Letters 25B, 5 (1967).

[21]T. T. S. Kuo and G. E. Brown, Nucl. Phys. A114, 241

(1968).
[22]R. C. Bearse, J. R. Comfort, J. P. Schiffer, M. M. Stautberg, and J. C. Stoltzfus, Phys. Rev. Letters 23, 864 (1969).
[23]P. W. M. Glaudemans, G. Weichers, and P. J. Brussaard, Nucl. Phys. 56, 548 (1964).

PHYSICAL REVIEW C VOLUME 3, NUMBER 5 MAY 1971

Spectroscopy of V^{50} with Direct (d, t) and (d, α) Reactions*

R. DelVecchio, W. W. Daehnick, D. L. Dittmer,† and Y. S. Park‡
Nuclear Physics Laboratory, University of Pittsburgh, Pittsburgh, Pennsylvania 15213
(Received 16 December 1970)

About 50 levels of V^{50} below 3.2 MeV have been studied with 9- to 15-keV resolution via the $V^{51}(d,t)V^{50}$, $Cr^{52}(d,\alpha)V^{50}$, and $Ti^{48}(He^3,p)V^{50}$ reactions. Angular distributions were taken (at 16 MeV) for the $V^{51}(d,t)$ reactions and (at 17 MeV) for $Cr^{52}(d,\alpha)V^{50}$. (d,t) and (d,α) l values were extracted by comparison with distorted-wave Born-approximation calculations. For most of the levels seen, direct-reaction selection rules lead to narrow limits for the final-state spins, and in a few cases to unique J^π assignments. The spectroscopic information for the lowest levels was compared with shell-model predictions, and qualitative agreement was found. The lowest negative-parity states seen were above 2 MeV. Little $2p$ strength was found in the pickup experiments, and strong suppression of (d,α) transitions to $J^\pi=(\text{even})^+$ states suggests that the low-lying states of V^{50} are predominantly of $(f_{7/2})^n$ configuration. However, a comparison with the (d,α) spectrum for the particle-hole conjugate nucleus Sc^{46} shows that these nuclei are more dissimilar than a simple $(f_{7/2})^n$ model would suggest.

I. INTRODUCTION

The low-lying states of the odd-odd nucleus V^{50} have been described in simple shell-model terms as having the configuration $[(f_{7/2})_p^3(f_{7/2})_n^{-1}]_{J+}$ and this assumption formed the basis of a theoretical treatment by McCullen, Bayman, and Zamick (MBZ).[1] In this description the particle-hole conjugate nucleus Sc^{46} is predicted to have the same spectrum as V^{50} for positive-parity states. A previous $V^{51}(p,d)V^{50}$ study showed[2] that the $f_{7/2}$ spectroscopic strengths of the low-lying states in V^{50} have a distribution which is quite similar to the theoretical prediction. A more detailed comparison could not be made, because the V^{50} spins were not known except for the ground state. More recently, a $Ti^{50}(p,n\gamma)V^{50}$ study[3] has suggested spin assignments for the first four excited states of V^{50}, and a $V^{50}(p,p')$ study has determined the energy levels of V^{50} with 8-keV resolution up to 3.75-MeV excitation.[4]

In this paper, we report independent level-energy assignments up to about 3.2-MeV excitation, as well as detailed $V^{51}(d,t)V^{50}$ and $Cr^{52}(d,\alpha)V^{50}$ angular distributions for about 50 of these levels.[5]

II. EXPERIMENTAL PROCEDURES

A. Energy Assignments

Four high-resolution $Cr^{52}(d,\alpha)V^{50}$ spectra were taken with photographic plates in the focal plane of the Pittsburgh split-pole spectrograph. Three of these were taken at $E_d=12$ MeV with $\theta=12$, 40, and 50° while one was taken at $E_d=17$ MeV for $\theta=12°$. In addition a $Ti^{48}(He^3,p)V^{50}$ spectrum was taken at $E_{He^3}=18$ MeV, $\theta=12°$. Excitation energies were calculated using a computer code which is based on an empirical calibration of the spectrograph. As a check, a $Cr^{52}(d,\alpha)V^{50}$ spectrum and a $Cu^{63}(d,\alpha)Ni^{61}$ spectrum were taken on the same plate with identical focal-plane settings, and the well-known[6] levels of Ni^{61} were used for calibration. Good internal agreement was obtained for level energies based on these different methods. Our final level energy assignments were based on a weighted average with more weight given to the Ni^{61} comparison spectrum method than to the others. The estimated systematic (scale) uncertainty is $\lesssim 0.2\%$. One of the (d,α) plate spectra is shown in Fig. 1. Independent level energies were obtained from $V^{51}(d,t)V^{50}$. Although these measurements provided superior resolution (~9 keV), (d,t) energies are listed only for close-lying doublets, since the position-sensitive counter calibrations[7] were subject to larger errors. The V^{50} excitation energies obtained are listed and compared with other work[3,4,8-10] in Table I. The weighted energy averages fall well within the errors of our (d,α) excitation energies and are used in all other tables and figures.

B. $V^{51}(d,t)V^{50}$ Angular Distributions

The $V^{51}(d,t)V^{50}$ reaction was investigated at a